Measurement of the proton electromagnetic form factors at BABAR

Vladimir Druzhinin

NSU/BINP, Novosibirsk

On behalf of the BABAR collaboration

PHIPSI13

International Workshop on e+e- Collisions from Phi to Psi

Rome, September 9-12, 2013

$e^+e^- \to p\bar{p}$ cross section

$$\sigma(s) = \frac{4\pi\alpha^2\beta C(s)}{3s}\left(|G_M(s)|^2 + \frac{2m_p^2}{s}|G_E(s)|^2\right), \quad s = 4E_b$$

C is the Coulomb factor ➡ The cross section is nonzero at threshold.

G_E and G_M are the electric and magnetic form factors, $G_E(0)=1$, $G_M(0)=2.79$.

From the measured cross section, a combination of the squared form factors can be extracted. We define the effective form factor:

$$|F_p(s)| = \sqrt{\frac{|G_M(s)|^2 + (2m_p^2/s)|G_E(s)|^2}{1 + 2m_p^2/s}}$$

At large energies the G_E term is suppressed as $1/E^2$ and $|F_p| \approx |G_M|$.

The ratio of the form factors $|G_E/G_M|$ can be determined from the analysis of the proton polar-angle distribution.

$$\frac{d\sigma}{d\Omega}(s,\theta) = \frac{\alpha^2\beta C(s)}{4s}\left(|G_M(s)|^2(1+\cos^2\theta) + \frac{4m_p^2}{s}|G_E(s)|^2\sin^2\theta\right)$$

At threshold $|G_E(4m_p^2)| = |G_M(4m_p^2)|$.

Previous e^+e^- experiments

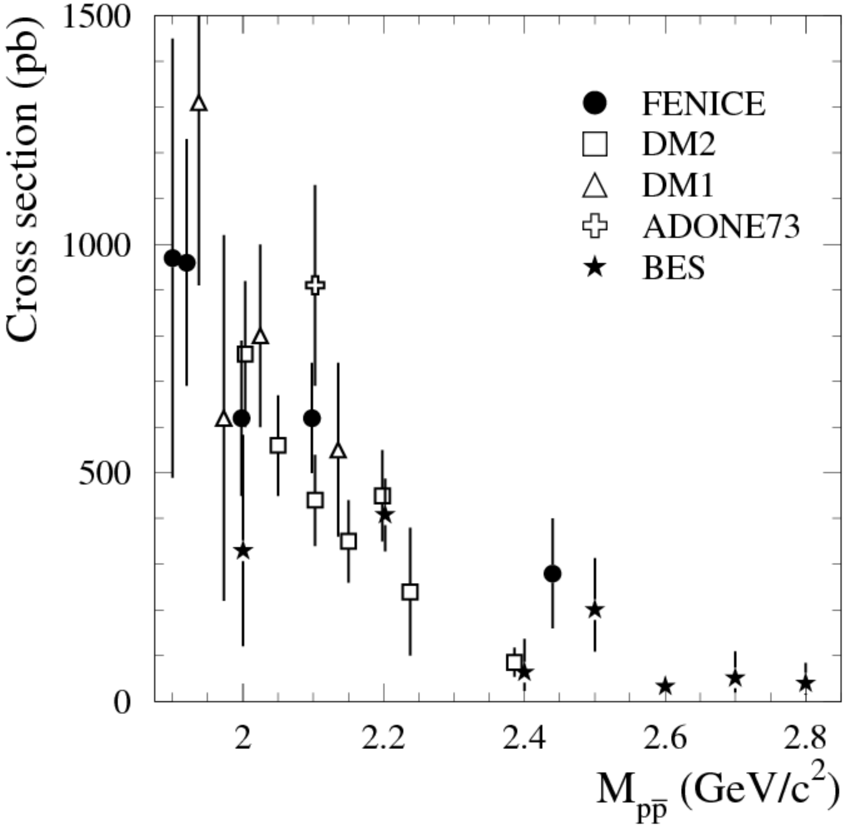

Below 3.2 GeV: ADONE73 (1973), DM1(1979), DM2(1983,1990), FENICE(1994), BES(2005).

Statistical accuracy of these measurements is (20-30)%.

Limited statistics do not allow to extract the G_E/G_M ratio from the analysis of the angular distribution.

Proton-antiproton collisions

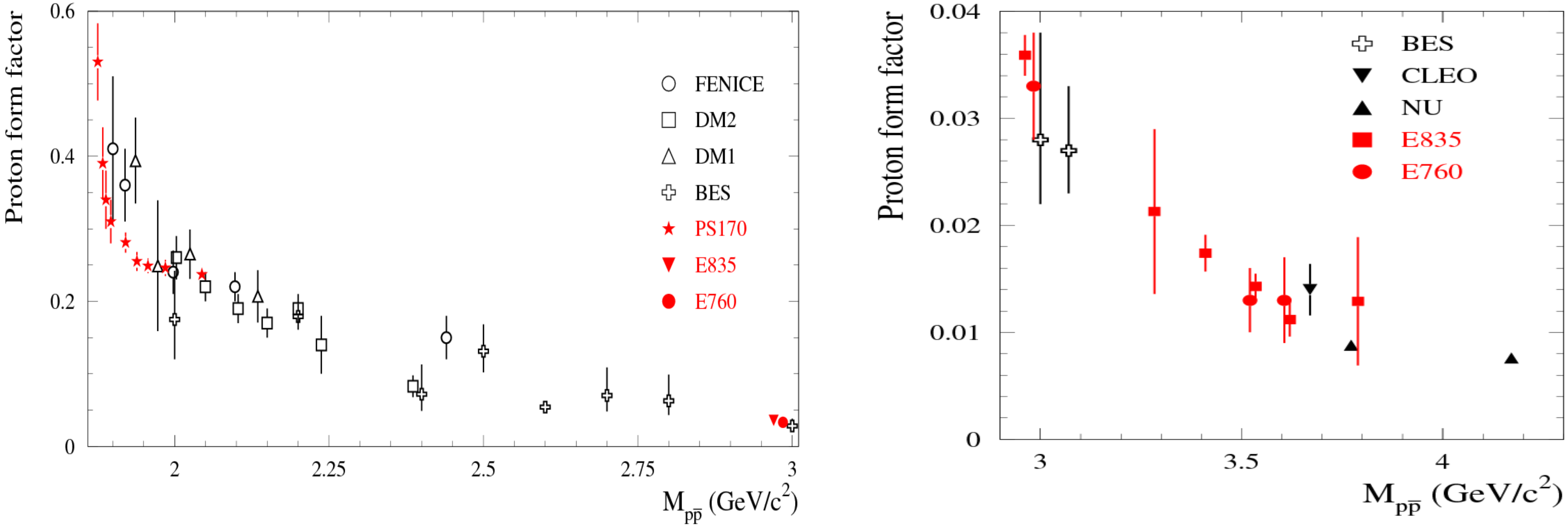

Near threshold data were obtained in PS170 experiment at the antiproton storage ring LEAR (CERN):

✓steep growth of the form factor near threshold,

✓the ratio $|G_E/G_M|$, measured with 30% accuracy in five energy points, agrees with unity.

Above 3 GeV measurements were performed at FNAL (E835 and E760).

The very precise points marked “NU” (Phys. Rev. Lett. 110 (2013) 022002) were obtained using CLEO data (~1 fb) collected at 3.77 and 4.17 GeV.

ISR method

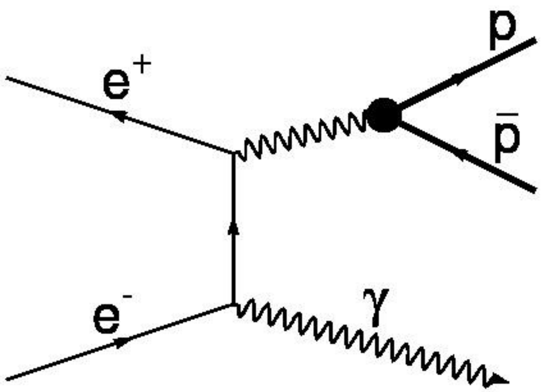

The mass spectrum of the proton-antiproton system in the reaction $e^+e^- \to p\bar{p}\gamma$ is related to the cross section for the nonradiative process $e^+e^- \to p\bar{p}$.

$$\frac{d\sigma_{e^+e^-\to p\bar{p}\gamma}}{dm\, d\cos\theta} = \frac{2m}{s} W(s,x,\theta)\, \sigma_{e^+e^-\to p\bar{p}}(m), \quad x = \frac{2E_\gamma}{\sqrt{s}} = 1 - \frac{m^2}{s}$$

The function $W(s,x,\theta)$ is calculated in QED. It describes angular ($1/\sin^2\theta$ at $\theta \gg m_e/\sqrt{s}$) and energy ($1/x$) distributions of the ISR photon.

ISR method

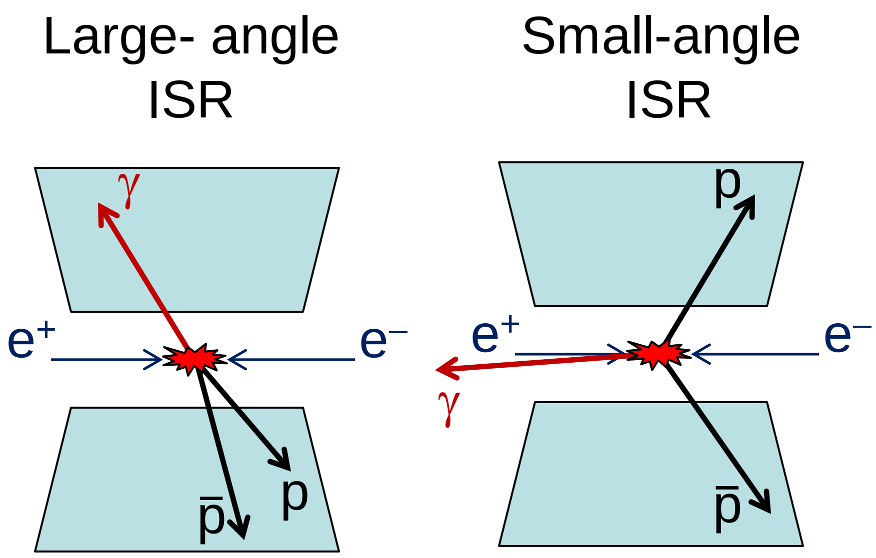

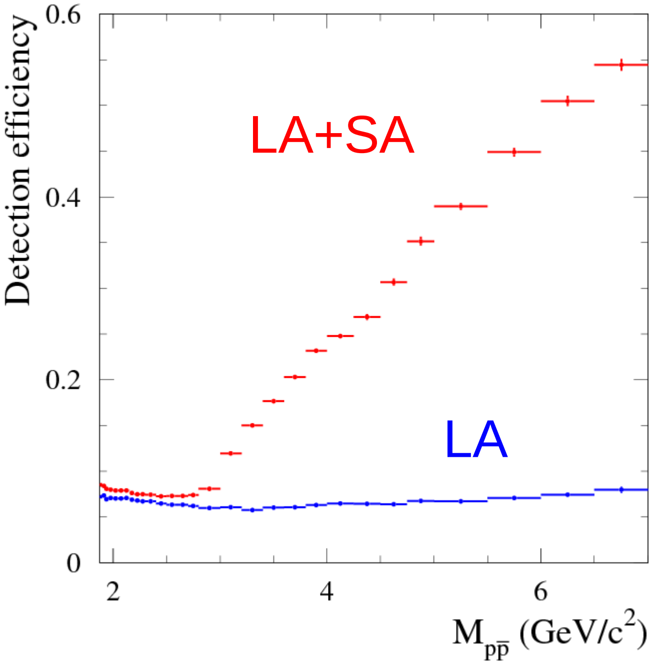

The ISR photon is emitted predominantly along the beam axis. The produced hadronic system is boosted against the ISR photon. Due to limited detector acceptance the mass region below 3 GeV can be studied only with detected photon (about 10% of ISR events).

Above 3 GeV statistics can be significantly increased by using small-angle ISR.

Advantages of the ISR method

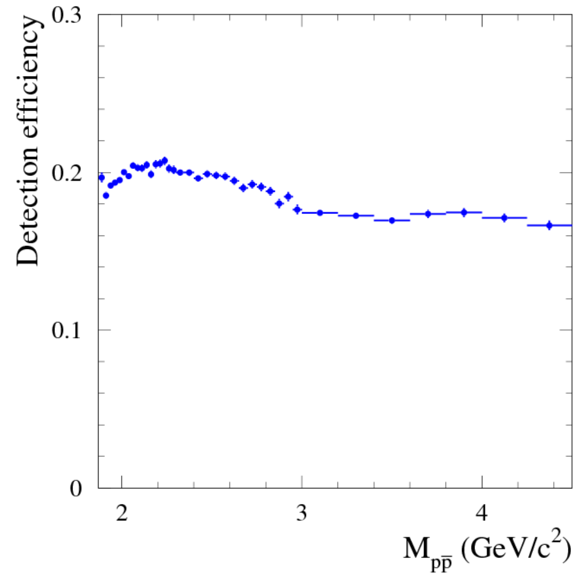

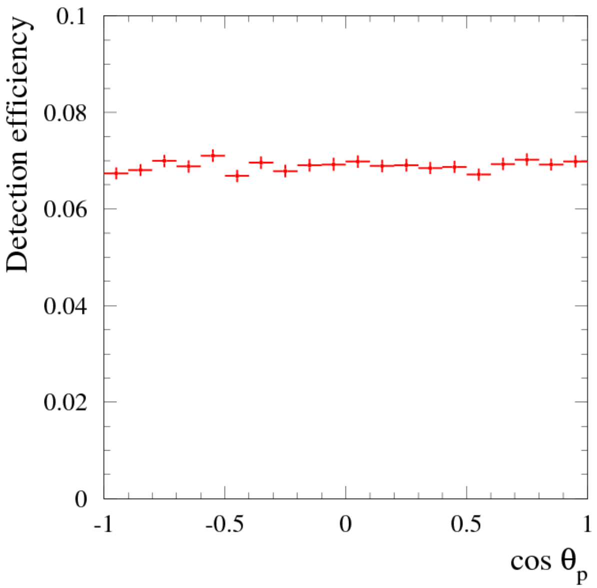

✓A wide energy region is studied in a single experiment.

The effective ISR luminosity (pb^{-1}/GeV) increases with mass, partly compensating a decrease of the measured cross section.

✓ A low dependence of the detection efficiency on the hadronic invariant mass

Measurement near and above threshold with the same selection criteria.

✓ A low dependence of the detection efficiency on hadron angular distributions (in the hadron rest frame).

For protons this significantly increases sensitivity for measurements of the G_E/G_M ratio.

BABAR detector

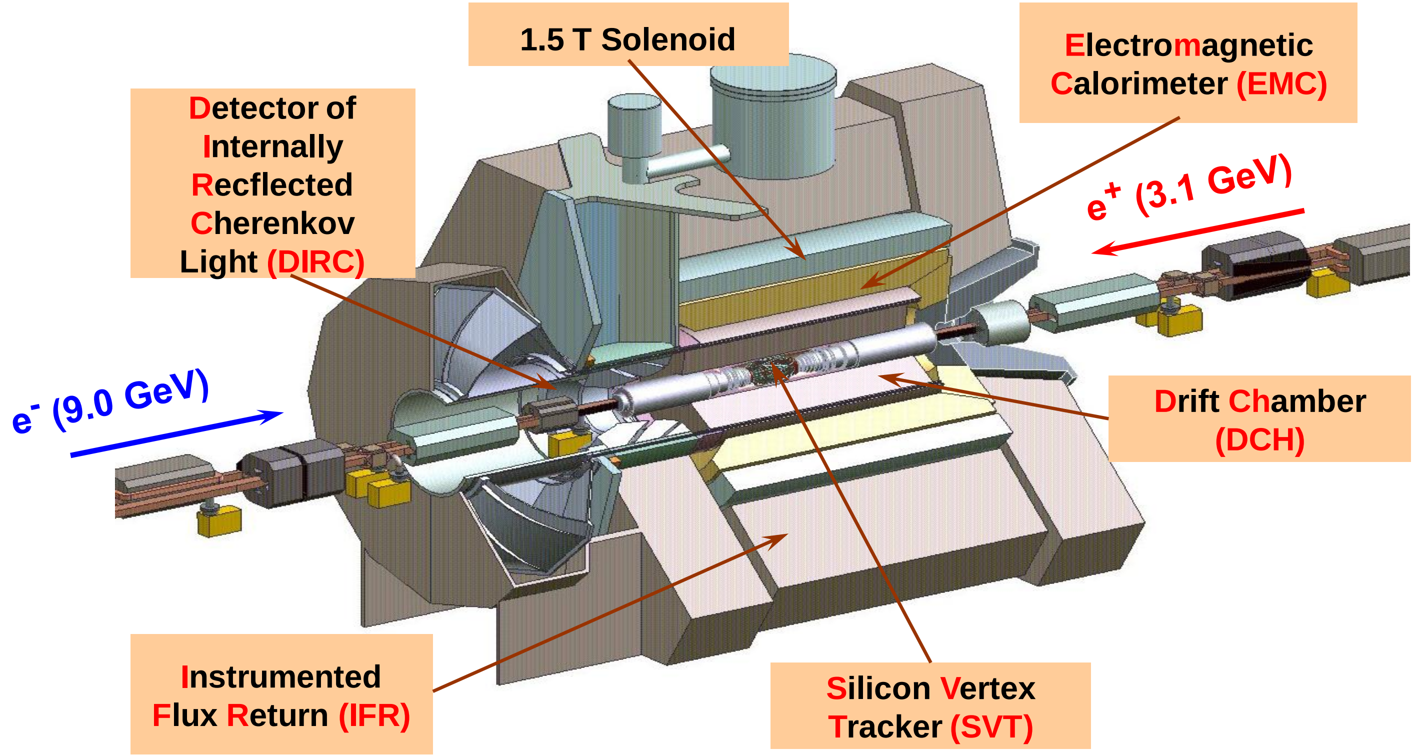

The full data sample collected at and near $\Upsilon(4S)$: 469 fb^{-1}.

The LA analysis is published in

Phys. Rev. D **87**, (2013) 092005,

Phys. Rev. D **73**, (2006) 012005 – 232 fb^{-1}.

The SA analysis is in **arXiv:1308.1795**

LA event selection

All final particles must be detected and well reconstructed.

✓2 tracks of opposite charges originating from the interaction point and identified as protons (25.8° < θ < 137.5°).

✓A photon candidate with $E_{c.m.}$ > 3 GeV (20.0° < θ < 137.5°).

✓A kinematic fit to the $e^+e^- \to h^+h^-\gamma$ hypothesis (h=p,K) is performed with requirements of energy and momentum conservation. $\chi^2_p < 30,\ \chi^2_K > 30$

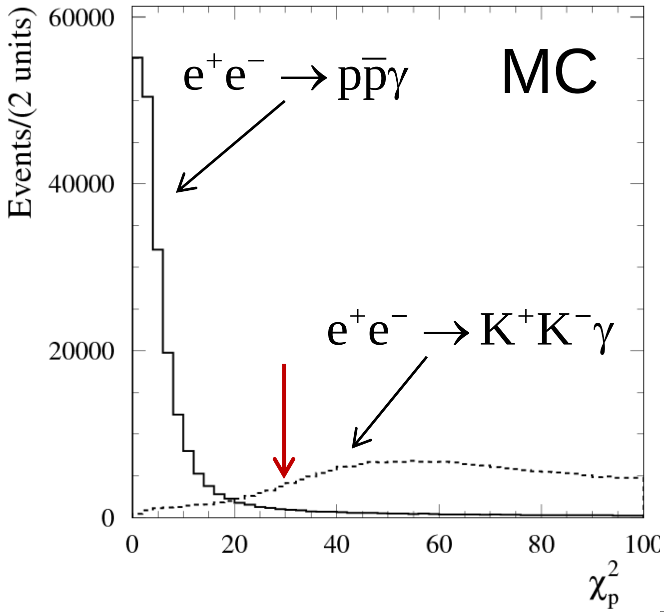

Backrounds from $e^+e^- \to \pi^+\pi^-\gamma$, $\mu^+\mu^-\gamma$, $K^+K^-\gamma$ exceed signal by 2-3 orders of magnitude.

These backgrounds are suppressed by the PID requirement and χ^2 cuts by a factor of 10^6 for pions and muons, and 3×10^5 for kaons.

Background for LA selection

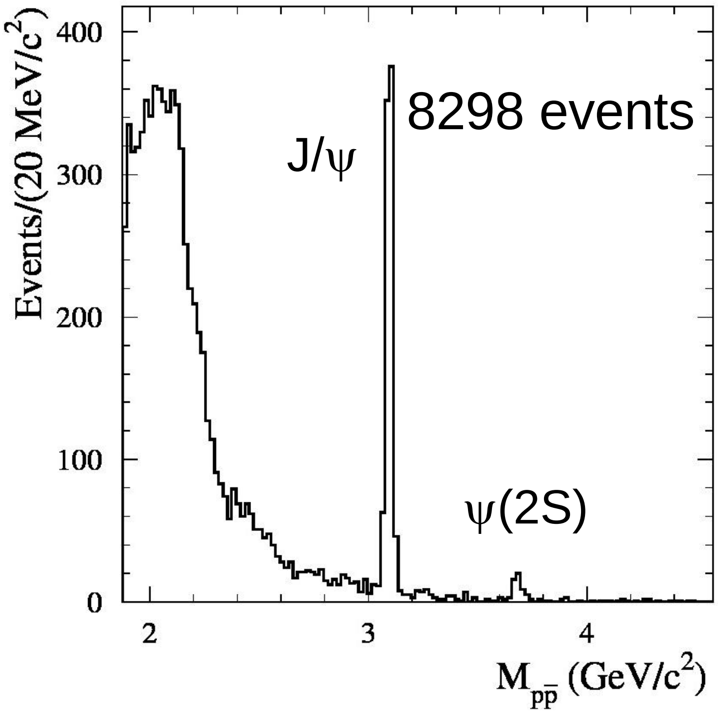

- The main background arises from $e^+e^- \to p\bar{p}\pi^0$ events with an undetected low-energy photon or with merged photons from the π^0 decay.
- This background is estimated from a control sample of $e^+e^- \to p\bar{p}\pi^0$ events.
- Increases from 5% at M_{pp}< 2.5 GeV to 50% at 4 GeV.
- All observed data events above 4.5 GeV are explained by this background.

data	$pp\gamma$	$pp\pi^0$	ISR and e^+e^-
8298	**7741 ± 113**	**448 ± 42**	**109 ± 30**

Background from e^+e^- annihilation processes other than $e^+e^- \to p\bar{p}\pi^0$ and ISR processes such as $e^+e^- \to p\bar{p}\pi_0\gamma$, $p\bar{p}2\pi_0\gamma$ is estimated using difference of the χ^2 distributions for signal and background events and subtracted.

SA event selection

✓2 tracks of opposite charge originating from the interaction point and identified as protons (25.8° < θ < 137.5°).

✓ $P_T < 0.15$ GeV/c

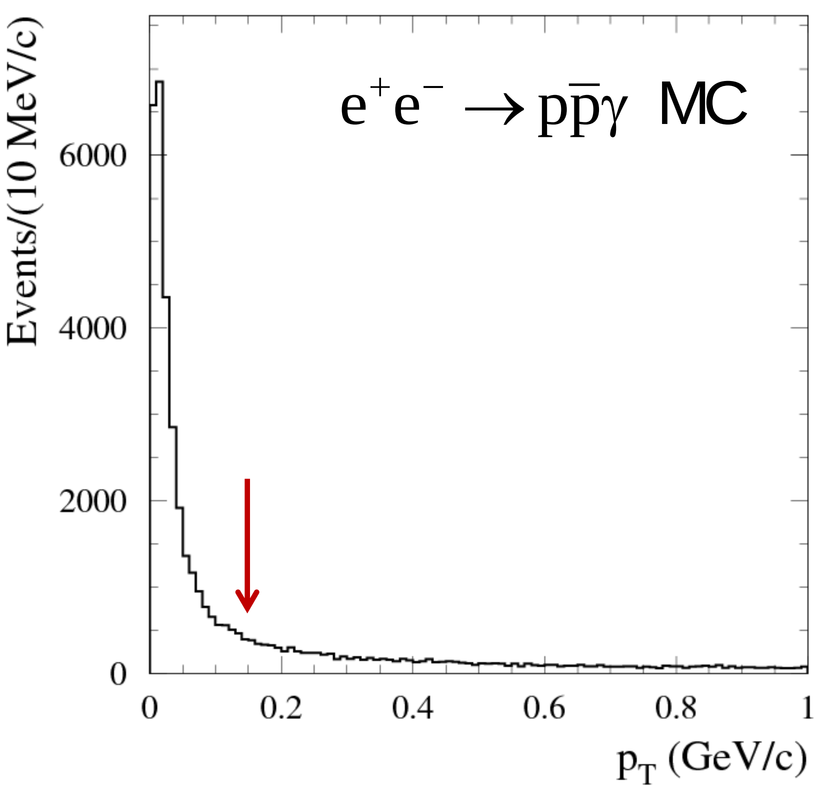

✓ $|M^2_{rec}| < 1$ GeV^2/c^4

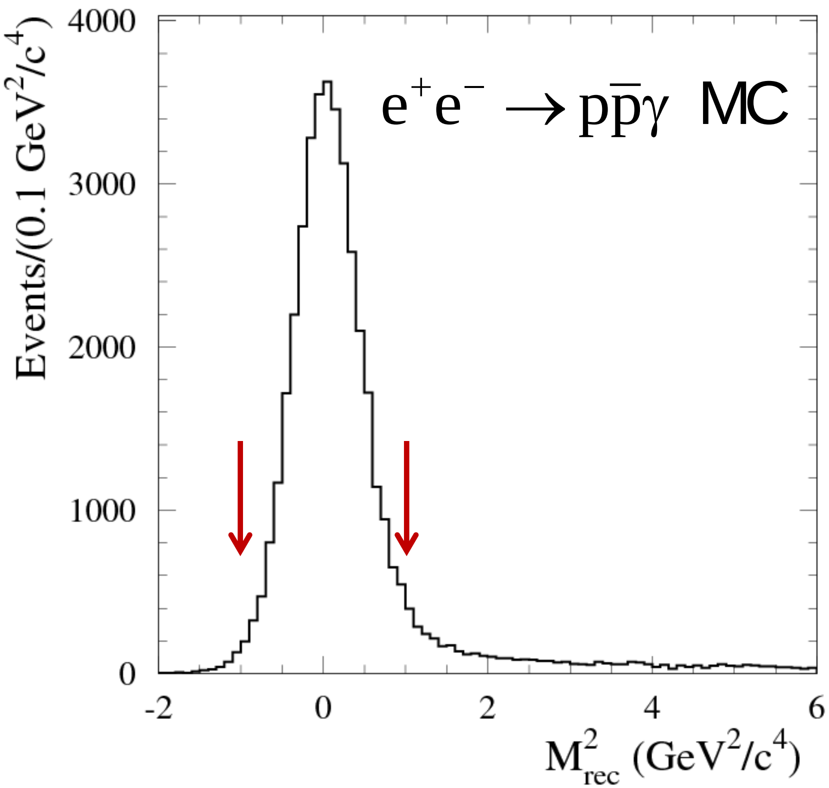

Background for SA ISR

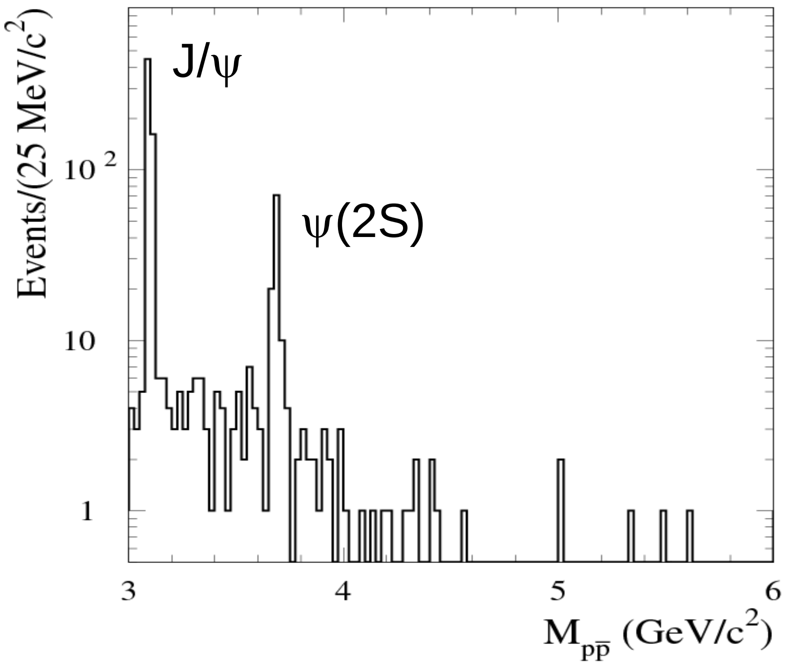

- The total number of selected events is 845.
- The number of nonresonant events is 149.
- No events are observed with mass above 6 GeV/c^2.

Data	$\mu\mu\gamma$	2-photon	ISR
149	< 1	1.6 ± 09	6.3 ± 3.5

➢The dominant background process is $e^+e^- \to p\bar{p}\pi^0\gamma$

➢The main background in our large-angle ISR analysis from $e^+e^- \to p\bar{p}\pi^0$ is found to be negligible.

Angular distribution

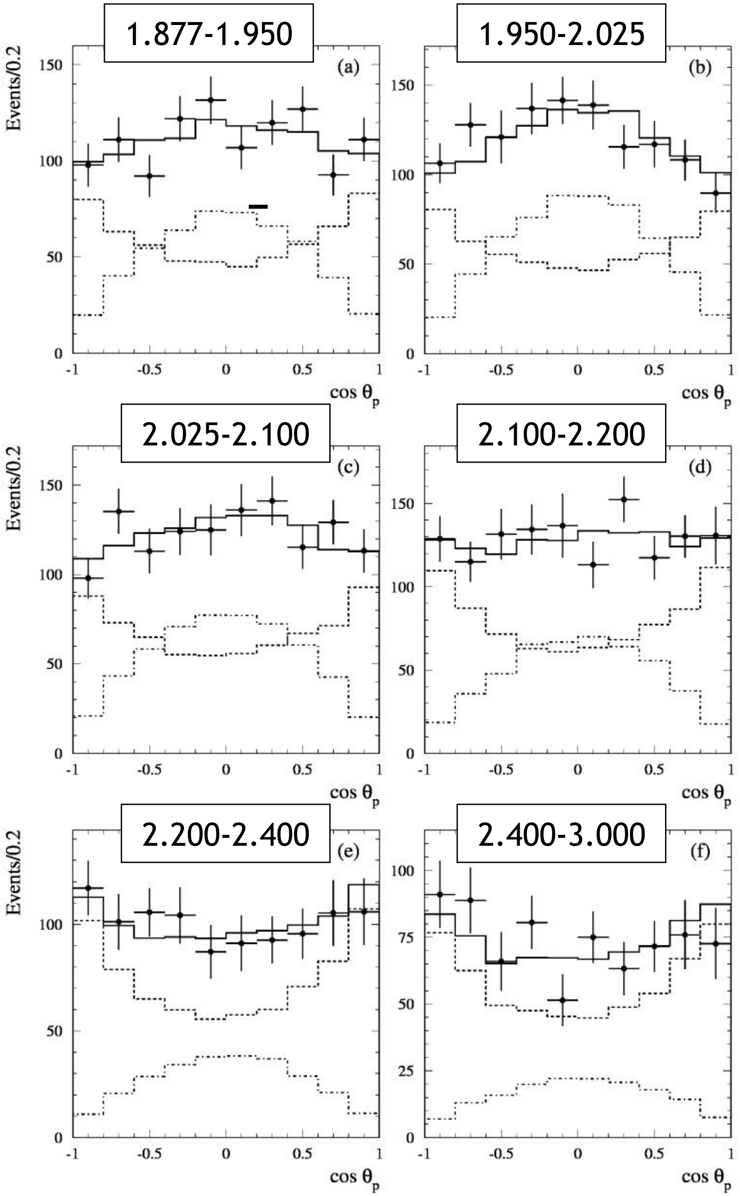

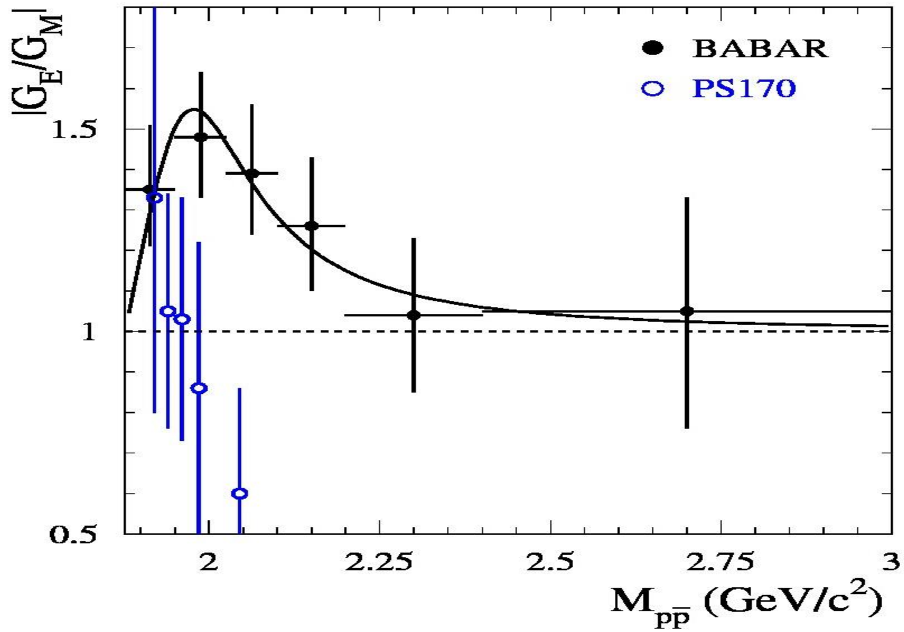

- θ_p is the angle between the proton momentum in the pp̄ rest frame and the momentum of pp̄ system in the e^+e^- c.m. frame.
- The distribution is fitted by a sum of histograms obtained from two simulated event samples, one with G_E=0 and other with G_M=0.
- These distributions are close to $1+\cos^2\theta_p$ and $\sin^2\theta_p$.

Asymmetry in the angular distribution

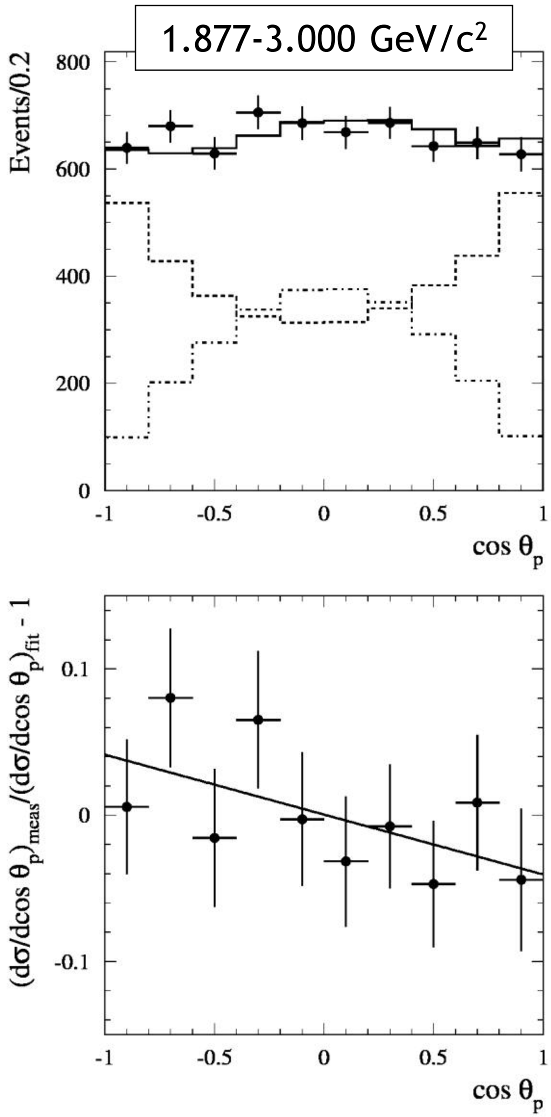

- The asymmetry is absent in lowest order ($\gamma^* \to p\bar{p}$). It arises from higher-order contributions (soft extra ISR and FSR interference, two-photon exchange). Measuring the asymmetry we control the higher-order contributions.
- Our simulation uses a model with one-photon exchange. The asymmetry in the simulated distribution is due to an asymmetry in the detection efficiency.
- We analyze the difference between the measured and fitted distributions.
- The slope is -0.041±0.026±0.005
- The integral asymmetry

$$A = \frac{\sigma(\cos\theta_p > 0) - \sigma(\cos\theta_p < 0)}{\sigma(\cos\theta_p > 0) + \sigma(\cos\theta_p < 0)} = -0.025 \pm 0.014 \pm 0.003$$

Measured cross section

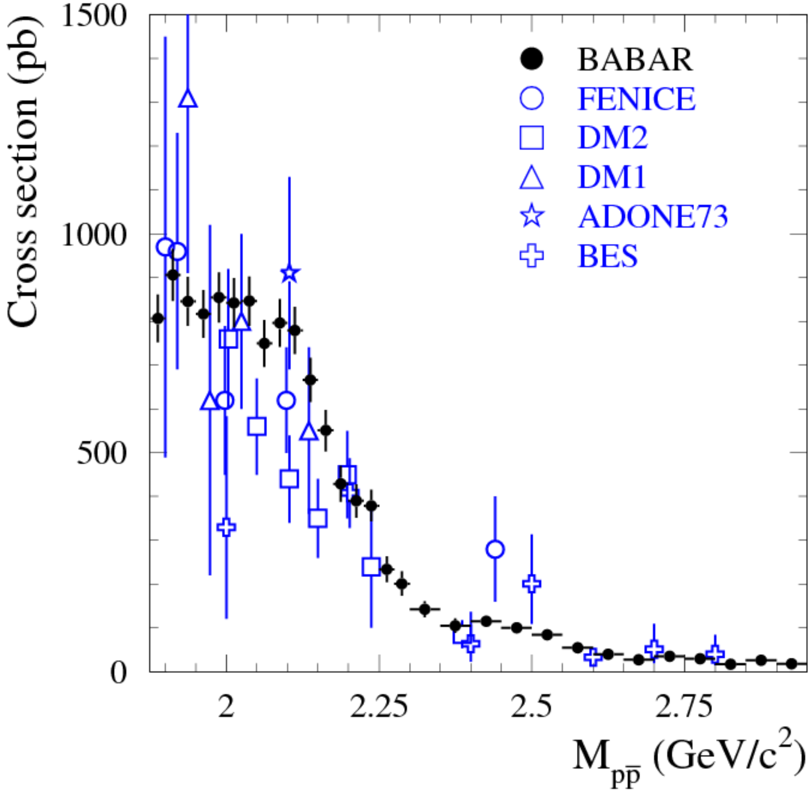

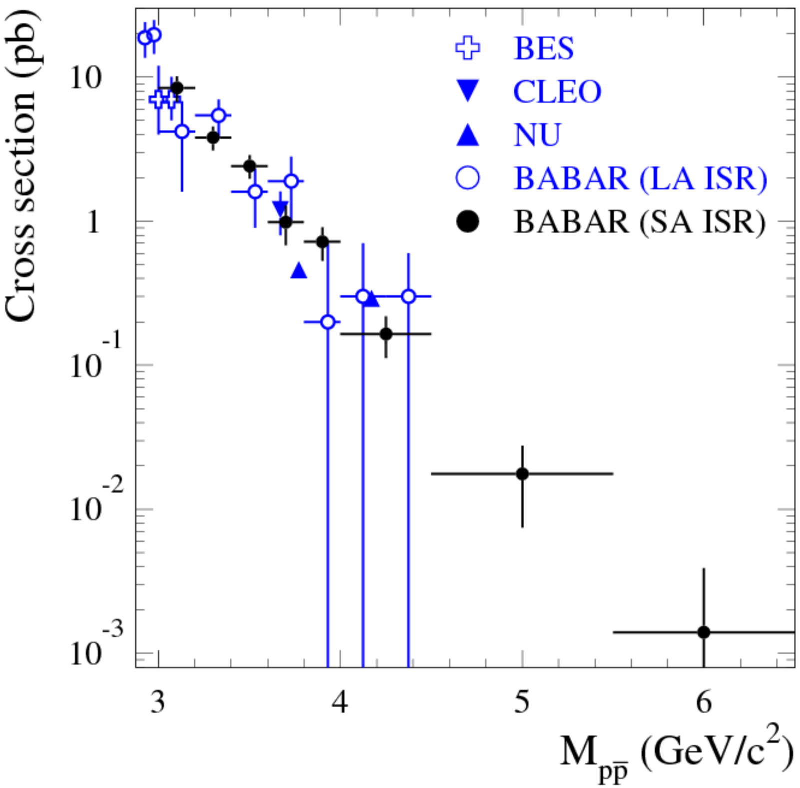

Mass-independent systematic uncertainty is 4-5% for large-angle ISR. For small-angle ISR it decreases from 16% at 3 GeV to 6% at 4.5 GeV.

✓ In the mass region under study the cross section changes by about six orders of magnitude.

✓Our data are in reasonable agreement with previous measurements

✓ We improve accuracy and extend the mass region of measurements.

Effective proton form factor

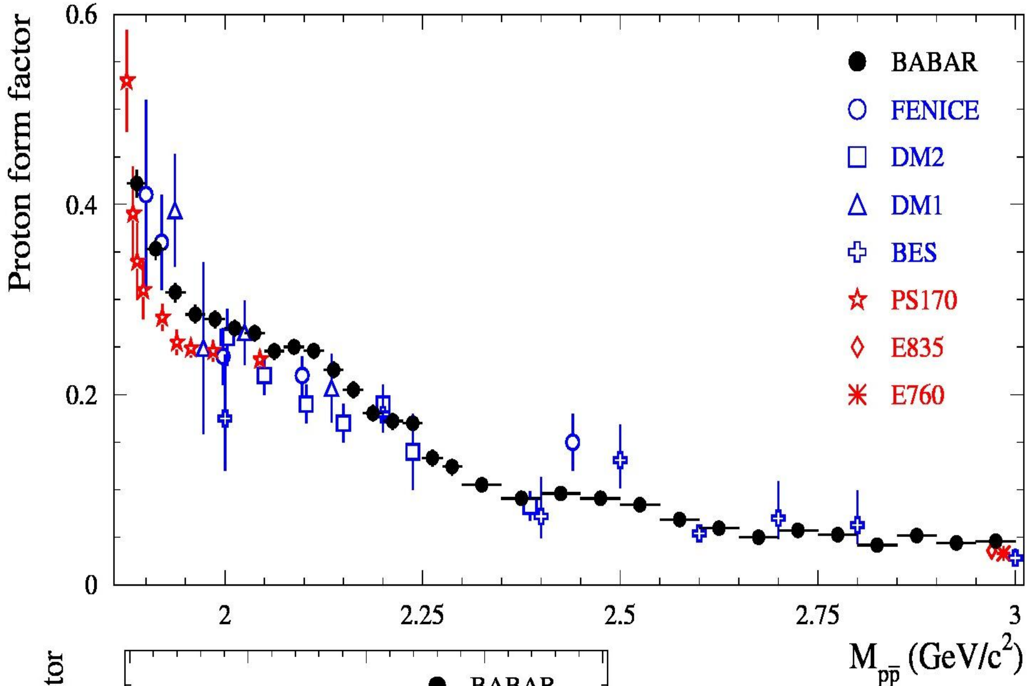

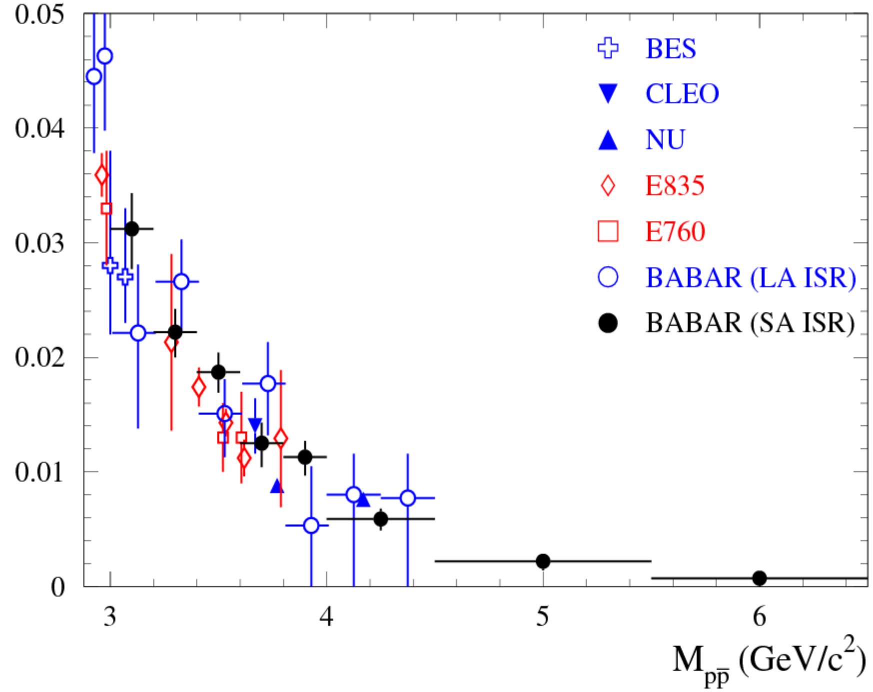

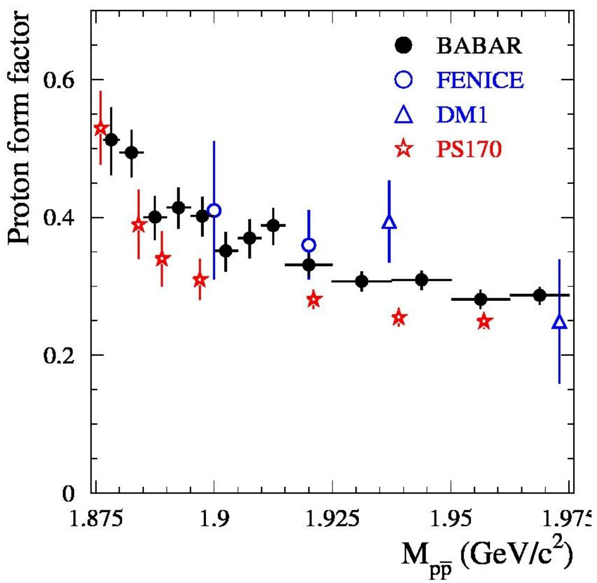

- A steep falloff and GE/GM $\neq$ 1 near threshold are explained by nucleons' final state interaction.
- A complex step-like behavior far of threshold (2 or even 3 steps at 2.2, 2.55, 3 GeV/c^2) is not described by existing models.

QCD-motivated fit

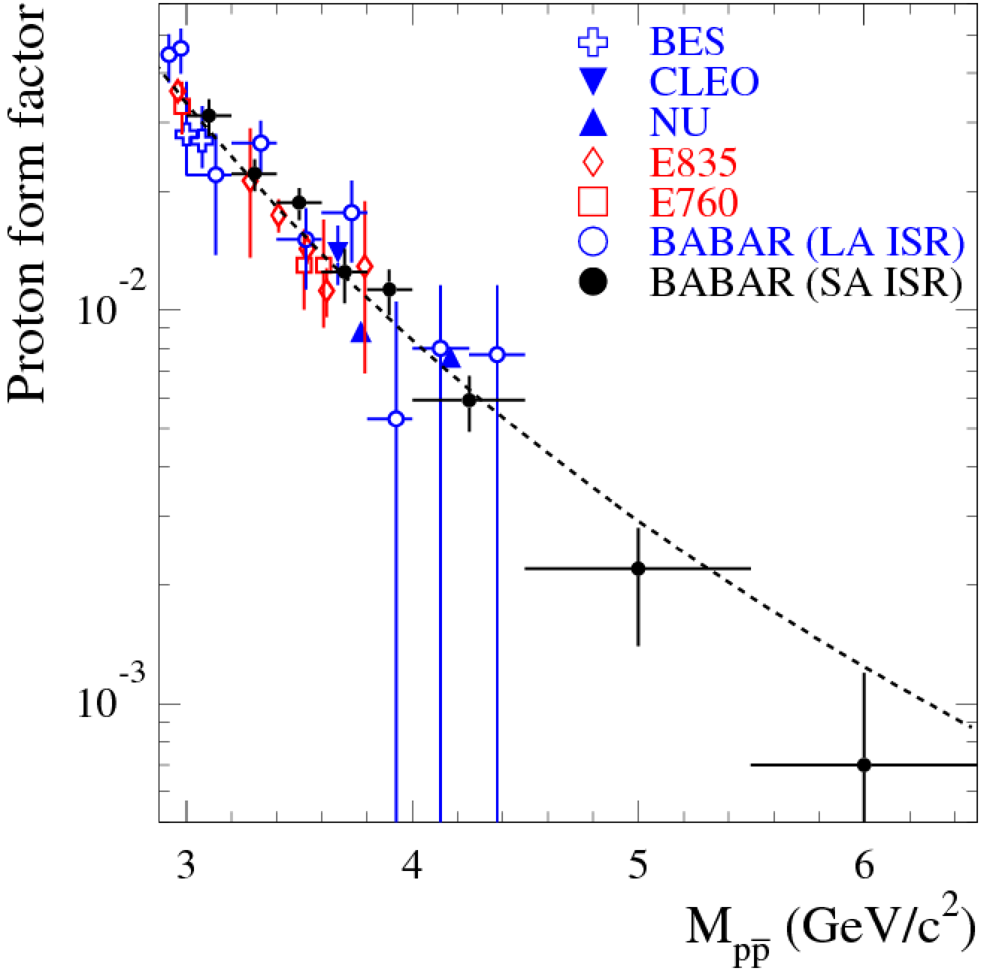

$$G_M \sim \frac{\alpha_s^2(m^2)}{m^4} \sim \frac{C}{m^4 \ln^2(m^2/\Lambda^2)}$$

✓ All the data above 3 GeV except the two "NU" points are well described by this function.

✓ Adding the "NU" points change the fit χ^2/ν from 17/24 to 54/26.

✓ Our data shows that the form factor decreases in agreement with the asymptotic QCD prediction or even faster above 4.5 GeV.

The local deviations of the "NU" points from the global fit may be result of the $\psi(3770)$ and $\psi(4160)$ resonance contributions.

Comparison with the space-like G_M

Data points with largest errors were excluded

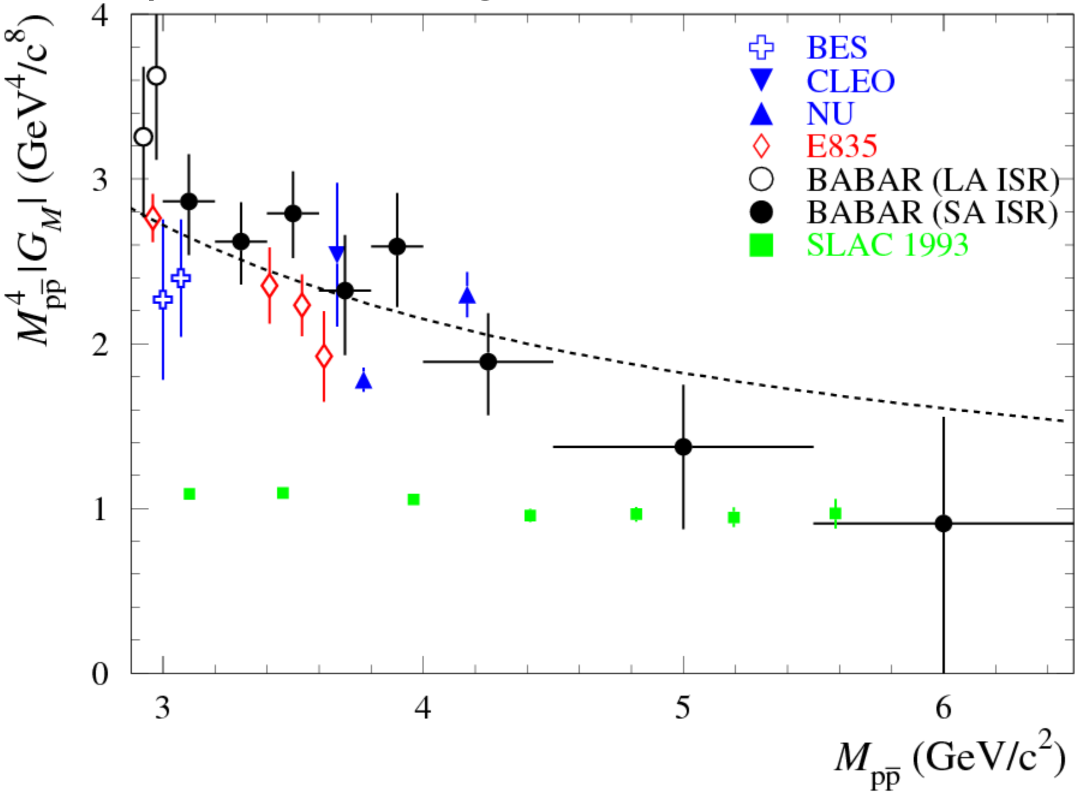

- The points "SLAC 1993" represent data on the space-like magnetic form factor measured in ep scattering as a function of $\sqrt{-q^2}$.
- The asymptotic values of the space- and time-like form factors are expected to be the same.

- In the mass region from 3.0 to 4.5 GeV the time-like form factor is about two-three times larger than the space-like one.
- The new BABAR SA ISR measurements give an indication that the difference between the time- and space-like form factors decreases with mass increase.

J/ψ and ψ(2S) decays

LA ISR

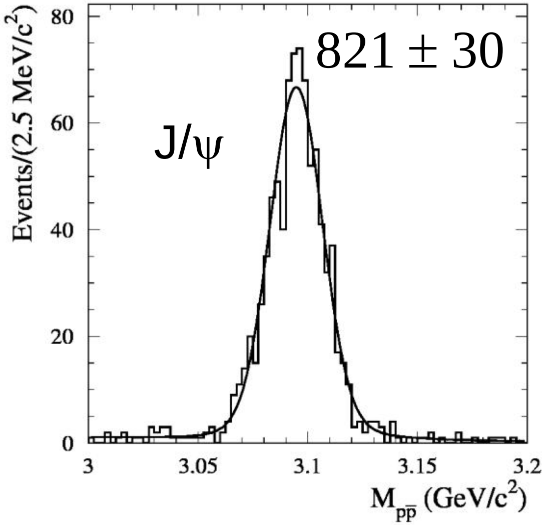

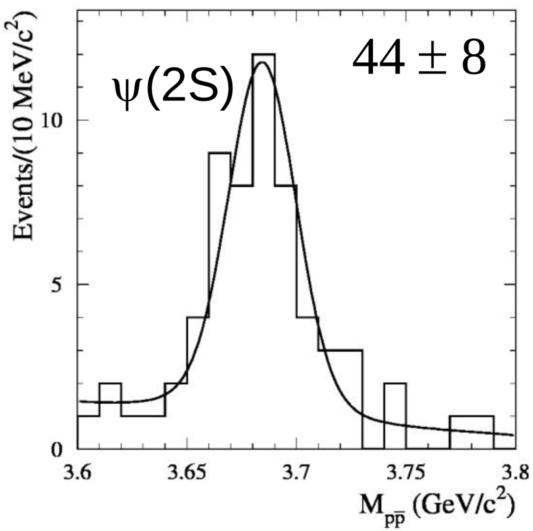

SA ISR

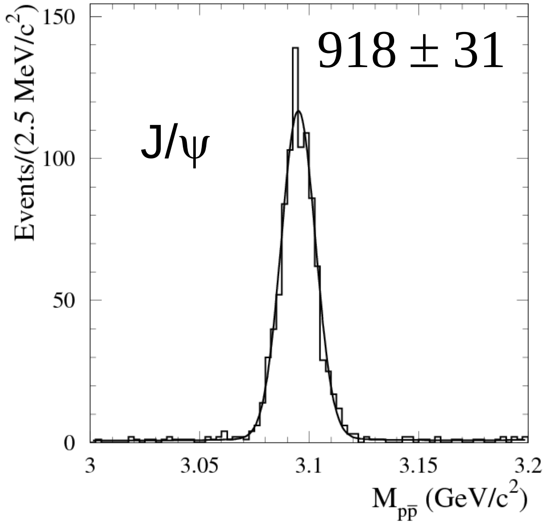

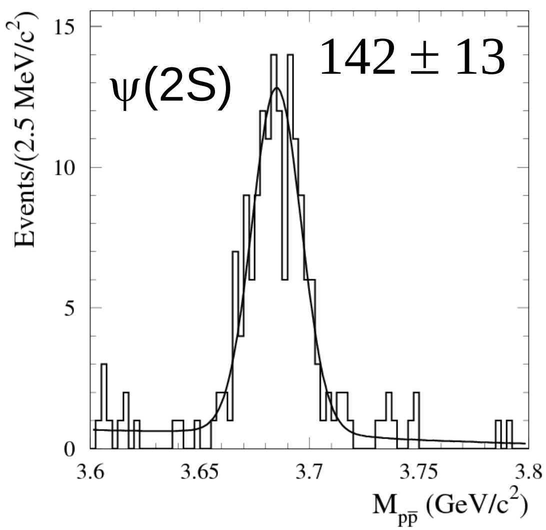

	$B(J/\psi \to p\bar{p}) \times 10^3$
SA	$2.33 \pm 0.08 \pm 0.09$
LA	$2.04 \pm 0.07 \pm 0.07$
PDG	2.120 ± 0.029

	$B(\psi(2S) \to p\bar{p}) \times 10^4$
SA	$3.14 \pm 0.28 \pm 0.18$
LA	$2.86 \pm 0.51 \pm 0.09$
PDG	2.75 ± 0.12

Summary

- The $e^+e^- \to p\bar{p}$ cross section and the proton effective form factor have been measured from threshold up to 6.5 GeV using the full BABAR data sample.
- The form factor has complex mass dependence. There are a near-threshold steep falloff and a step-like behavior at higher masses.
- The $|G_E/G_M|$ ratio has been measured from threshold to 3 GeV/c^2. A large deviation of this ratio from unity is observed below 2.2 GeV/c^2.
- Asymmetry in the proton angular distribution have been measured.
- At masses above 3 GeV the observed decrease of the form factor agrees with the asymptotic dependence $\alpha_s^2(m)/m^4$ predicted by QCD.